

Published in final edited form as:

*J Neuroimaging*. 2015 January ; 25(1): 62–67. doi:10.1111/jon.12124.

## Corpus callosum atrophy correlates with gray matter atrophy in patients with multiple sclerosis

Eric C. Klawiter, MD, MSc<sup>1</sup>, Antonia Ceccarelli, MD, PhD<sup>2</sup>, Ashish Arora, MD<sup>2</sup>, Jonathan Jackson, PhD<sup>2</sup>, Sonya Bakshi<sup>2</sup>, Gloria Kim, BA<sup>2</sup>, Jennifer Miller, BA<sup>2</sup>, Shahamat Tauhid, MD<sup>2</sup>, Christian von Gizycki<sup>2</sup>, Rohit Bakshi, MD, MA<sup>2</sup>, and Mohit Neema, MD, MA<sup>2</sup>

<sup>1</sup>Department of Neurology, Massachusetts General Hospital, Harvard Medical School, Boston, MA, USA

<sup>2</sup>Department of Neurology, Brigham and Women's Hospital, Laboratory for Neuroimaging Research, Partners MS Center, Harvard Medical School, Boston, MA, USA

### Abstract

**Objective**—Atrophy of the corpus callosum is a recognized characteristic of multiple sclerosis (MS). We describe a new reliable method for measuring corpus callosum atrophy and correlate this with global cerebral atrophy measures.

**Methods**—Whole brain 3T MRI was performed in 38 relapsing-remitting MS subjects and 21 healthy controls (HC). Brain global gray and white matter volumes were segmented with SPM8. The contour of the corpus callosum was outlined on the midline of 3D T1-weighted images by a semi-automated edge-detection technique to determine the corpus callosum area (CCA). Normalized CCA was correlated with other brain atrophy measures in MS subjects.

**Results**—CCA was disproportionately lower in MS subjects vs. HC (20.1% mean decrease,  $p < 0.001$ ), with a large effect size ( $d = 0.62$ ) when compared with global atrophy measures. In MS subjects, CCA correlated with brain parenchymal fraction ( $r = 0.55$ ,  $p < 0.001$ ) and gray matter

---

Correspondence: Mohit Neema, MD, Brigham and Women's Hospital, Suite 602, One Brookline Pl, Brookline MA 02445, mneema@bwh.harvard.edu, 617-726-7643.

The first and corresponding authors take full responsibility for the data, the analyses and interpretation, and the conduct of the research. The first and corresponding authors guarantee the accuracy of the references. The funding source had no role in the study design or in the collection, analysis and interpretation of data. The Methods section includes a statement that IRB approval as been obtained for the use of human subjects for this study.

### Disclosures

Dr. Klawiter has received research funding from Roche. Dr. Klawiter has received consulting fees and/or speaking honoraria from Biogen Idec, Bayer Healthcare, Genzyme Corporation, and Teva Neuroscience.

Dr. Ceccarelli has nothing to disclose.

Dr. Arora has nothing to disclose.

Dr. Jackson has nothing to disclose.

Sonya Bakshi has nothing to disclose.

Gloria Kim has nothing to disclose.

Jennifer Miller has nothing to disclose.

Dr. Tauhid has nothing to disclose.

Christian Vongizycki has nothing to disclose.

Dr. Bakshi has nothing to disclose.

Dr. Neema has nothing to disclose.

fraction ( $r=0.45$ ,  $p=0.005$ ) but not white matter fraction ( $r=0.18$ ,  $p=0.29$ ). An inverse correlation with FLAIR hyperintense lesion volume ( $r=-0.40$ ,  $p=0.01$ ) was detected for CCA.

**Conclusion**—Measurement of atrophy of the corpus callosum can have sensitivity as a useful imaging biomarker in patients with MS, even in patients with low disability levels. Both gray and white matter involvement in MS contribute to corpus callosum atrophy.

## Keywords

multiple sclerosis; corpus callosum; atrophy

## Introduction

Cerebral atrophy is a clinically relevant manifestation of multiple sclerosis (MS) pathology.<sup>1,2</sup> Atrophy can occur early in the disease course and is considered a substrate for clinical disability and cognitive dysfunction.<sup>3</sup> Atrophy occurs differentially in the gray matter (GM) and white matter (WM) in MS and may contribute to various aspects of MS-related cognitive dysfunction.<sup>4</sup>

Examples of GM structures most vulnerable to early atrophy in MS include the thalamus and the hippocampus.<sup>5, 6</sup> The corpus callosum, the compact WM bundle connecting the two hemispheres, represents a WM region of distinct interest because of the predilection for MS pathology.<sup>7, 8</sup> The exact mechanism of corpus callosal atrophy is not clearly understood and may include the direct result of focal lesions, Wallerian degeneration from MS pathology in adjacent WM areas, or a secondary effect of neurodegenerative processes in GM. Prior studies have associated corpus callosum atrophy with the level of disability in MS.<sup>9, 10</sup> Furthermore, the corpus callosum is implicated in cognitive dysfunction in MS and its involvement may disrupt inter-hemispheric connectivity.<sup>11,12,13,14,15,16</sup> The relationship between corpus callosum damage and cognitive dysfunction can be shown even in benign MS.<sup>17</sup>

In this study, we sought to describe a new method to assess callosal atrophy from 3T MRI and characterize its relationship to global cerebral atrophy.

## Methods

### Standard Protocol Approvals, Registrations, and Patient Consents

Informed consent was obtained from all subjects under the Partners Institutional Review Board.

### Subjects

General demographic and clinical data were obtained from 38 relapsing-remitting (RR) MS subjects and 21 age-matched healthy controls (HC) (Table 1). All MS subjects met McDonald diagnostic criteria.<sup>18</sup> Other inclusion criteria included no relapse or corticosteroid use within 4 weeks prior to study entry (to avoid transient confounding effects on MRI) and absence of another major medical disorder. At the time of enrollment, MS subjects were on treatment with glatirimer acetate ( $n=16$ ), interferon beta ( $n=16$ ) or no disease-modifying

therapy (n=6). All subjects underwent a 25 foot timed walk and the Expanded Disability Status Scale (EDSS) examination by MS specialist neurologists. Healthy controls for this study were recruited as described previously.<sup>19</sup>

### Image Acquisition

All subjects underwent whole brain MR imaging at 3T (Signa; GE Healthcare, Milwaukee, Wisconsin), using the same scanning protocol. Imaging was performed using a multichannel head-only phased array coil. Brain imaging sequences included the following:

1. Axial FLAIR: TR = 9000 ms, TE = 151 ms, TI = 2250 ms, section thickness = 2 mm (70 sections, no gap), matrix size =  $256 \times 256$ , pixel size =  $0.976 \times 0.976$  mm, number of signal averages = 1, acquisition time ~ 9 minutes.
2. Coronal 3D Modified Driven Equilibrium Fourier Transform (MDEFT)<sup>20</sup>: TR = 7.9 ms, TE = 3.14 ms, flip angle =  $15^\circ$ , section thickness = 1.6 mm (124 sections, no gap), matrix size =  $256 \times 256$ , pixel size =  $0.938 \times 0.938$  mm, number of signal averages = 1, acquisition time ~ 7.5 minutes.

All image analysis was performed in a blinded manner, without knowledge of group assignment or clinical information.

### Corpus Callosum Area Determination

An expert observer (ECK) blinded to clinical information performed corpus callosum area (CCA) determination. The MDEFT images were re-sampled (1.6 mm slice thickness) in the sagittal anterior commissure (AC) to posterior commissure (PC) plane in a new, in-house developed method to accurately represent the midline of the corpus callosum using Jim software (v5.0, Xinapse Systems). A mid-sagittal slice was selected in the AC-PC plane for further analysis. Intensity normalization was applied with a maximal intensity of 1.2 times the intensity of the splenium of the corpus callosum (a relatively high intensity region of the corpus callosum) on MDEFT images to help standardize edge detection of the corpus callosum. The contour of the corpus callosum was outlined by a semi-automated edge-detection technique to determine the CCA (Figure 1). The intra- and inter-rater observer (2 observers - ECK and AA) variability was assessed by intraclass correlation coefficient (ICC) analysis in a subset of randomly chosen 6 MS patients.

### Global Cerebral Image Segmentation and Lesion Determination

MDEFT scans were deskulled using a semi-automated tool in the Jim software package. The intracranial volume (ICV) was used to normalize all CNS volume measurements.

Manually skull stripped MDEFT images were first brought into approximate alignment with the ICBM template, then bias-field corrected, spatially normalized and automatically segmented into GM, WM, and CSF probability maps using the unified segmentation model implemented in the segmentation routine of SPM8<sup>21</sup> running in Matlab (version 2009a, The MathWorks, Inc., Natick, MA, USA). Within manual outlines of the intracranial cavities, mutually exclusive masks for each tissue were derived from SPM8 tissue probability maps as described previously.<sup>22</sup> Estimates of WM volume (WMV), GM volume (GMV), CSF volume (CSFV), and brain parenchymal volume (BPV = WMV + GMV) were automatically

derived from SPM8 generated segmentations after corrections for T1-hypointense lesion-related misclassifications and deep GM underestimation as previously described.<sup>23</sup> These values were used to compute normalized compartment volumes: WM fraction (WMF = WMV/ICV), GM fraction (GMF = GMV/ICV), and brain parenchymal fraction [BPF = (WMV + GMV)/ICV].

Whole brain FLAIR lesion volume (FLV) was obtained by a semi-automated edge-finding method based on local thresholding as previously described.<sup>24</sup>

### Statistical Analysis

Corpus callosum area measurements were normalized by ICV to the 2/3 power. Corpus callosum area and volumetric measures were compared between MS subjects and HC using multiple linear regression (with age and sex as covariates). Effect size was determined using Cohen's *d*, defined as the difference between the two means divided by the standard deviation of the data.<sup>25</sup> Corpus callosum area was correlated with other brain atrophy measures in MS subjects using Pearson's correlation coefficient, with FLV using Spearman's correlation coefficient, and with EDSS using Kendall's tau-b. A *p* value of <0.05 was considered significant. Statistical analyses utilized the Statistical Package for the Social Sciences (SPSS, v. 21, Chicago, IL).

## Results

### Corpus Callosum Area

Intra-rater reliability (ICC=0.98) and inter-rater reliability (ICC=0.96) were high and included all aspects of the new CCA method, starting with resampling. When determining differences between MS and controls, age was added to the model to control for any confounding effect. Group differences in imaging outcomes are shown in Table 2. Corpus callosum area was lower in MS subjects vs. HC (20.1% mean decrease, *p*<0.001) (Figure 2). The effect size for CCA (*d*=0.62) was greater than any of the global atrophy measures (BPF, 2.3% decrease, *p*=0.004, *d*=0.39; GMF, 2.0% decrease, *p*=0.036, *d*=0.20; WMF, 2.8% decrease, *p*=0.222, *d*=0.23). Thus, the corpus callosum showed selective disproportionate atrophy vs. global cerebral measures in patients with RRMS.

### MRI Correlates of Corpus Callosum Atrophy

Corpus callosum area did not correlate with BPF, GMF or WMF in control subjects (all *p* >0.05, data not shown). Figure 3 shows simple scatterplots detailing the relationship between CCA and other MRI measures in MS subjects. Corpus callosum area correlated with BPF (*r*=0.55, *p*<0.001) and GMF (*r*=0.45, *p*=0.005), but not WMF (*r*=0.18, *p*=0.29). An inverse correlation with FLV (*r*=-0.40, *p*=0.01) was detected for CCA, indicating a relationship between WM lesions and corpus callosum degeneration.

### Clinical Correlates of Corpus Callosum Atrophy

There was a trend for correlation of CCA with EDSS score (tau=-0.23, *p*=0.06). Of the volumetric atrophy measures, only BPF correlated with EDSS (BPF, tau=-0.33, *p*=0.011; GMF, tau=-0.20, *p*=0.11; WMF, tau=0.20; *p*=0.11). Corpus callosum area did not correlate

with disease duration ( $r=0.05$ ,  $p=0.43$ ) or 25-foot timed walk ( $r=-0.19$ ,  $p=0.23$ ) in MS subjects. Only BPF correlated with 25-foot timed walk ( $r=0.40$ ,  $p=0.014$ ).

## Discussion

We describe an optimized method that reliably quantifies corpus callosum atrophy. We evaluated corpus callosum atrophy in relationship to common measures of whole brain and compartment-specific global cerebral atrophy in a group of HC and RRMS subjects. Corpus callosum area was disproportionately low in MS and displayed a larger effect size than other measures of atrophy. Corpus callosum atrophy correlated with BPF, GMF, WM lesions, and trended toward correlation with EDSS.

In the current study, we introduce a novel optimized approach to segmenting the corpus callosum. This was based on previous methods with the addition of image resampling and intensity normalization.<sup>10</sup> There are several possible ways of quantifying atrophy of the corpus callosum. Volumetric measures of the corpus callosum suffer from inexact determinations of the lateral margins of the corpus callosum. Several corpus callosum parcellation schemes have been used previously, but here we relied on cross sectional area of the entire corpus callosum.<sup>26</sup> Other methods have used 1-dimensional corpus callosum thickness to estimate corpus callosum atrophy in a simplified method that can be performed easily on clinical MRIs.<sup>16, 27</sup> Our new method is based on the notion that area measures in the mid-sagittal plane may reflect the total corpus callosum volume. With our technique, steps were taken, including resampling images, to analyze the exact mid-sagittal slice of corpus callosum in order to provide a reliable 2-dimensional quantitative outcome, CCA. We aimed to normalize CCA for head size using ICV, similar to methods used to normalize GMV and WMV to derive GMF and WMF. This method uses a resampled single sagittal slice, which offers the advantage of simplicity in measurement. Although only a single slice is used, the uniformity of the corpus callosum implies that a mid-sagittal slice should be representative. This led to a highly reliable estimation of corpus callosum volume, shown by high intra- and inter-class correlation. Although we have not as yet tested the longitudinal sensitivity of our methods, we hypothesize that this measure can be easily incorporated into therapeutic clinical trials and even clinical settings.

Even in a group of MS subjects with relatively low levels of disability, atrophy of the corpus callosum was significant, similar to other studies of early onset MS with mild disability.<sup>28</sup> In our study, corpus callosum atrophy was evident to a greater extent than other commonly derived global atrophy measures such as BPF, GMF and WMF. When compared to HC, the effect size of CCA in MS was greater than any other atrophy outcome evaluated. A different study examining CIS patients, showed that a >1% change in CCA over six months predicted conversion to clinically definite MS (CDMS).<sup>29</sup> In the same study, GM atrophy was not a predictor of conversion to CDMS and was not different between CIS and CDMS groups. This provides some evidence that the corpus callosum may be a sensitive tool to monitor the destructive aspects of the disease even in patients with mild disability and who are early in their disease course.

A strength of this study includes the correlation of CCA with other imaging outcomes. Surprisingly, corpus callosum atrophy correlated with GMF but not WMF, even though the corpus callosum makes up a component of the WM. It is possible this could reflect a technical limitation of measurement of WM atrophy, confounded by transient inflammatory and fluid-related changes.<sup>30</sup> Corpus callosum atrophy significantly correlated with FLV, suggesting a component of this atrophy may be related to WM disease and Wallerian degeneration. In the HC group, there was no association between CCA and any other volumetric measure. This suggests that corpus callosum atrophy occurs in concert with reductions in GMF, although may not be directly related to it. This finding is supported by a study by Bendfeldt et al. who assessed the association between WM lesion distributions and GM volume changes.<sup>31</sup> They found that WM lesion changes in the corpus callosum and optic radiations were associated with cortical GM volume reductions. Current understanding of cortical atrophy suggests that this process, perhaps related in part to cortical demyelination, may occur by a different mechanism than atrophy of the corpus callosum.<sup>32</sup> Mechanistically, our study suggests that both GM and WM processes contribute to corpus callosum atrophy.

Disability level trended toward correlation with CCA, unlike a previous study<sup>16</sup> using a different measure of corpus callosum atrophy; although the MS subjects we studied overall had a mild level of disability, limiting the range of disability levels studied. Even so, this adds to significance of corpus callosum changes demonstrated in this study.

This study was limited by its cross-sectional design. A logical extension of this study would include longitudinal study of change in CCA in conjunction with measuring changes in other atrophy outcomes in relationship to disability. Future studies may also want to investigate the relationship between CCA and regional (deep and cortical) gray matter volumes. Addition of cognitive testing would further strengthen the significance of these results.

In conclusion, measurement of atrophy of the corpus callosum can have sensitivity as an imaging outcome in patients with MS, even in patients with low disability levels. Reliable determination of corpus callosum atrophy is of importance because of the structure's known relationship with disability and cognitive dysfunction.

## Acknowledgments

### Funding:

Supported by grants from the National Institutes of Health [1K23NS078044-01 (ECK)] and the National Multiple Sclerosis Society (RG3798A2, RB).

## References

1. Miller DH, Grossman RI, Reingold SC, McFarland HF. The role of magnetic resonance techniques in understanding and managing multiple sclerosis. *Brain*. 1998; 121 (Pt 1):3–24. [PubMed: 9549485]
2. Ceccarelli A, Bakshi R, Neema M. MRI in multiple sclerosis: a review of the current literature. *Curr Opin Neurol*. 2012; 25:402–409. [PubMed: 22691759]

3. Riccitelli G, Rocca MA, Pagani E, et al. Cognitive impairment in multiple sclerosis is associated to different patterns of gray matter atrophy according to clinical phenotype. *Hum Brain Mapp.* 2011; 32:1535–1543. [PubMed: 20740643]
4. Sanfilipo MP, Benedict RH, Weinstock-Guttman B, Bakshi R. Gray and white matter brain atrophy and neuropsychological impairment in multiple sclerosis. *Neurology.* 2006; 66:685–692. [PubMed: 16534104]
5. Sicotte NL, Kern KC, Giesser BS, et al. Regional hippocampal atrophy in multiple sclerosis. *Brain.* 2008; 131:1134–1141. [PubMed: 18375977]
6. Houtchens MK, Benedict RH, Killiany R, et al. Thalamic atrophy and cognition in multiple sclerosis. *Neurology.* 2007; 69:1213–1223. [PubMed: 17875909]
7. Barnard RO, Triggs M. Corpus callosum in multiple sclerosis. *J Neurol Neurosurg Psychiatry.* 1974; 37:1259–1264. [PubMed: 4457618]
8. Giorgio A, Battaglini M, Rocca MA, et al. Location of brain lesions predicts conversion of clinically isolated syndromes to multiple sclerosis. *Neurology.* 2013; 80:234–241. [PubMed: 23223533]
9. Yaldizli O, Atefy R, Gass A, et al. Corpus callosum index and long-term disability in multiple sclerosis patients. *J Neurol.* 2010; 257:1256–1264. [PubMed: 20198382]
10. Vaneckova M, Kalincik T, Krasensky J, et al. Corpus callosum atrophy--a simple predictor of multiple sclerosis progression: a longitudinal 9-year study. *Eur Neurol.* 2012; 68:23–27. [PubMed: 22677920]
11. Rao SM, Bernardin L, Leo GJ, Ellington L, Ryan SB, Burg LS. Cerebral disconnection in multiple sclerosis. Relationship to atrophy of the corpus callosum. *Arch Neurol.* 1989; 46:918–920. [PubMed: 2757533]
12. Lowe MJ, Beall EB, Sakaie KE, et al. Resting state sensorimotor functional connectivity in multiple sclerosis inversely correlates with transcallosal motor pathway transverse diffusivity. *Hum Brain Mapp.* 2008; 29:818–827. [PubMed: 18438889]
13. Llufriu S, Blanco Y, Martinez-Heras E, et al. Influence of corpus callosum damage on cognition and physical disability in multiple sclerosis: a multimodal study. *PLoS One.* 2012; 7:e37167. [PubMed: 22606347]
14. Rossi F, Giorgio A, Battaglini M, et al. Relevance of brain lesion location to cognition in relapsing multiple sclerosis. *PLoS One.* 2012; 7:e44826. [PubMed: 23144775]
15. Bergendal G, Martola J, Stawiarz L, Kristoffersen-Wiberg M, Fredrikson S, Almkvist O. Callosal atrophy in multiple sclerosis is related to cognitive speed. *Acta Neurol Scand.* 2013; 127:281–289. [PubMed: 22988936]
16. Yaldizli O, Penner IK, Frontzek K, et al. The relationship between total and regional corpus callosum atrophy, cognitive impairment and fatigue in multiple sclerosis patients. *Mult Scler.* 2013
17. Mesaros S, Rocca MA, Riccitelli G, et al. Corpus callosum damage and cognitive dysfunction in benign MS. *Hum Brain Mapp.* 2009; 30:2656–2666. [PubMed: 19067325]
18. Polman CH, Reingold SC, Edan G, et al. Diagnostic criteria for multiple sclerosis: 2005 revisions to the “McDonald Criteria”. *Ann Neurol.* 2005; 58:840–846. [PubMed: 16283615]
19. Neema M, Guss ZD, Stankiewicz JM, Arora A, Healy BC, Bakshi R. Normal findings on brain fluid-attenuated inversion recovery MR images at 3T. *AJNR Am J Neuroradiol.* 2009; 30:911–916. [PubMed: 19369605]
20. Deichmann R, Schwarzbauer C, Turner R. Optimisation of the 3D MDEFT sequence for anatomical brain imaging: technical implications at 1.5 and 3 T. *Neuroimage.* 2004; 21:757–767. [PubMed: 14980579]
21. Ashburner J, Friston KJ. Unified segmentation. *Neuroimage.* 2005; 26:839–851. [PubMed: 15955494]
22. Chard DT, Griffin CM, Parker GJ, Kapoor R, Thompson AJ, Miller DH. Brain atrophy in clinically early relapsing-remitting multiple sclerosis. *Brain: a journal of neurology.* 2002; 125:327–337. [PubMed: 11844733]
23. Cohen AB, Neema M, Arora A, et al. The relationships among MRI-defined spinal cord involvement, brain involvement, and disability in multiple sclerosis. *J Neuroimaging.* 2012; 22:122–128. [PubMed: 21447024]

24. Stankiewicz JM, Glanz BI, Healy BC, et al. Brain MRI lesion load at 1.5T and 3T versus clinical status in multiple sclerosis. *J Neuroimaging*. 2011; 21:e50–56. [PubMed: 19888926]
25. Cohen, J. *Statistical Power Analysis for the Behavioral Sciences*. 2. Hillsdale, NJ: Lawrence Erlbaum Assoc; 1988.
26. Sampat MP, Berger AM, Healy BC, et al. Regional white matter atrophy--based classification of multiple sclerosis in cross-sectional and longitudinal data. *AJNR Am J Neuroradiol*. 2009; 30:1731–1739. [PubMed: 19696139]
27. Figueira FF, Santos VS, Figueira GM, Silva AC. Corpus callosum index: a practical method for long-term follow-up in multiple sclerosis. *Arq Neuropsiquiatr*. 2007; 65:931–935. [PubMed: 18094848]
28. Pelletier J, Suchet L, Witjas T, et al. A longitudinal study of callosal atrophy and interhemispheric dysfunction in relapsing-remitting multiple sclerosis. *Arch Neurol*. 2001; 58:105–111. [PubMed: 11176943]
29. Kalincik T, Vaneckova M, Tyblova M, et al. Volumetric MRI markers and predictors of disease activity in early multiple sclerosis: a longitudinal cohort study. *PLoS One*. 2012; 7:e50101. [PubMed: 23166826]
30. Bermel RA, Bakshi R. The measurement and clinical relevance of brain atrophy in multiple sclerosis. *Lancet Neurol*. 2006; 5:158–170. [PubMed: 16426992]
31. Bendfeldt K, Blumhagen JO, Egger H, et al. Spatiotemporal distribution pattern of white matter lesion volumes and their association with regional grey matter volume reductions in relapsing-remitting multiple sclerosis. *Hum Brain Mapp*. 2010; 31:1542–1555. [PubMed: 20108225]
32. Wegner C, Esiri MM, Chance SA, Palace J, Matthews PM. Neocortical neuronal, synaptic, and glial loss in multiple sclerosis. *Neurology*. 2006; 67:960–967. [PubMed: 17000961]



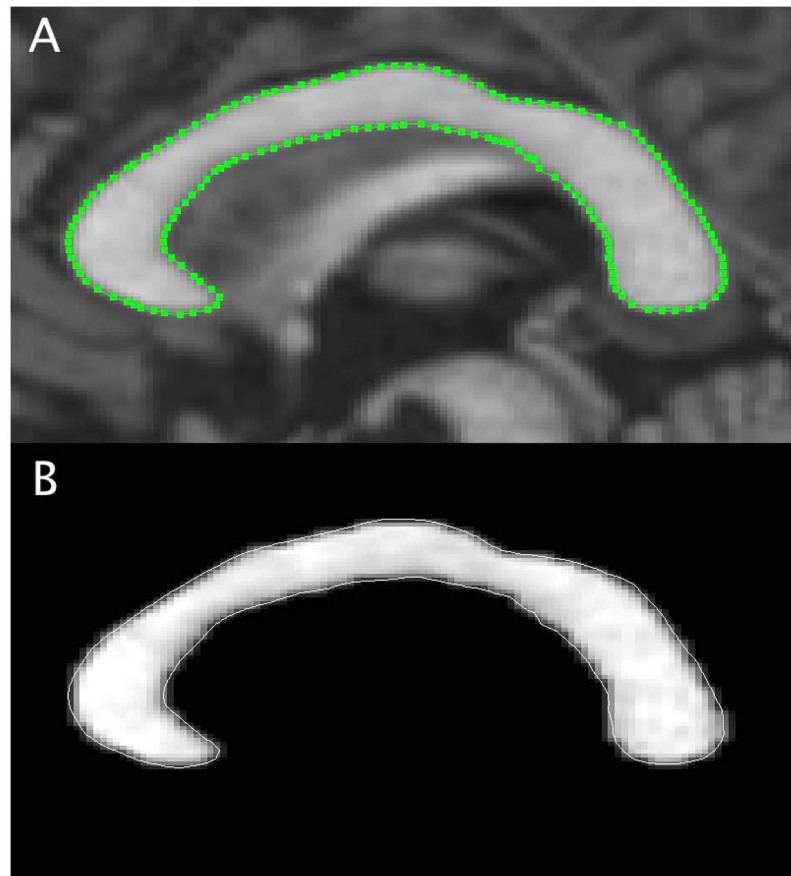


**Figure 1.** Corpus callosum area determination from 3D T1-weighted MDEFT images obtained with 3T MRI. A. Using a semi-automated edge detection method, an ROI is created for the midline of the corpus callosum. B. The corpus callosum is visualized as a masked view for cross sectional area determination.

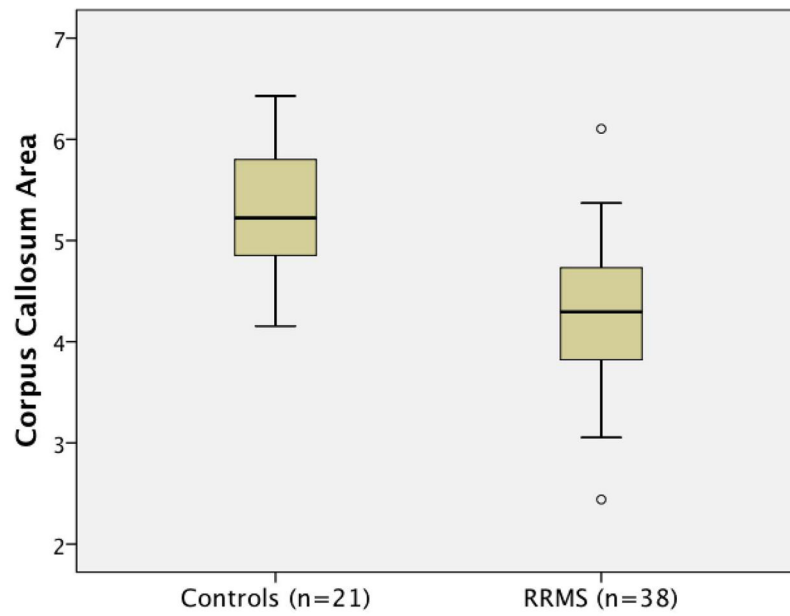


**Figure 2.**

Box plot of corpus callosum area by subject group. Corpus callosum area was lower in MS subjects vs. HC (20.1% mean decrease,  $p < 0.001$ ). Boxes represent 25th–75th percentiles. Whiskers represent two standard deviations from the mean. Outliers are represented by circles.

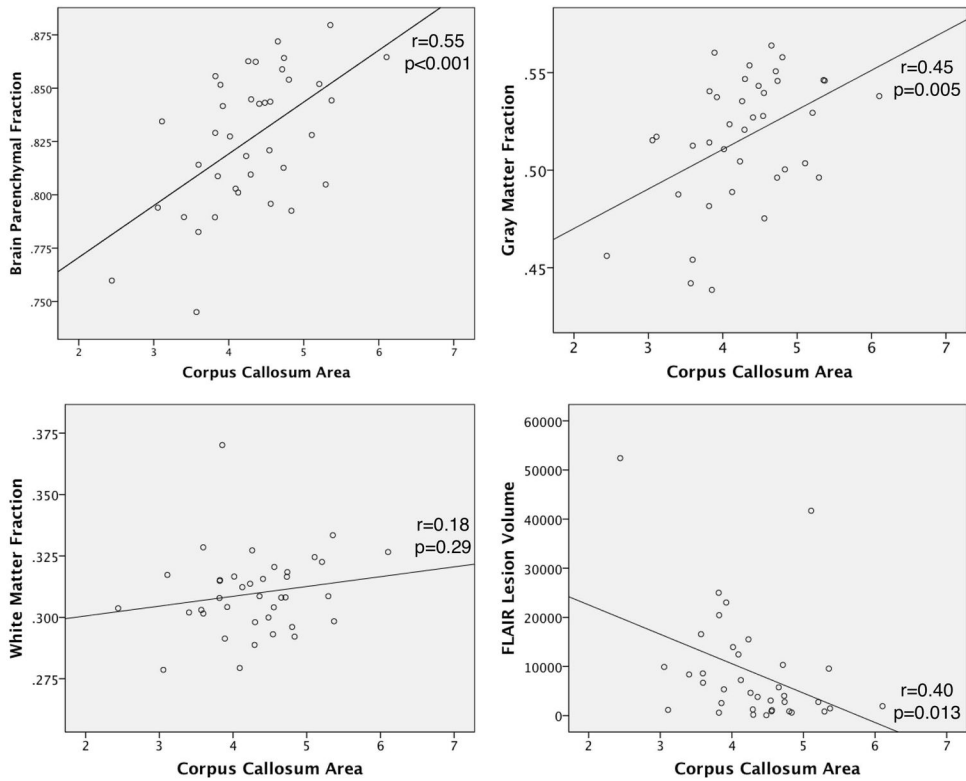


**Figure 3.**

Correlation of corpus callosum area (CCA) with brain parenchymal fraction (BPF), gray matter fraction (GMF), and white matter fraction (WMF). A scatterplot of CCA vs. BPF ( $r=0.55$ ,  $p<0.001$ ) and CCA vs. GMF ( $r=0.45$ ,  $p=0.005$ ) show moderate significant correlations. A scatterplot of CCA vs. WMF shows no correlation ( $r=0.18$ ,  $p=0.29$ ). FLV vs. CCA demonstrate an inverse correlation ( $r=-0.40$ ,  $p=0.013$ ).

**Table 1**

Demographic, clinical and MRI data

	<b>Healthy Controls</b>	<b>RRMS</b>
Subjects	21	38
Sex ratio (Males/Females)	5/16	13/25 (p=0.41)
Age (yrs), mean $\pm$ SD (range)	44 $\pm$ 6.8 (30–53)	40 $\pm$ 7.8 (21–53) (p=0.026)
Disease duration (yrs), mean $\pm$ SD (range)	N/A	8.0 $\pm$ 5.9 (1–28)
Median EDSS (range)	N/A	1.0 (0–3.5)
25-foot timed walk (seconds), mean $\pm$ SD (range)	N/A	4.1 $\pm$ 0.7 (2.9–6.5)
FLAIR lesion volume (mm <sup>3</sup> ), mean $\pm$ SD (range)	N/A	8848 $\pm$ 11453 (80–52411)

Key: N/A = Not applicable, EDSS = expanded disability status score, FLAIR = fluid attenuated inversion recovery, RRMS = relapsing-remitting multiple sclerosis.

**Table 2**

Differences in volumetric measures between controls and RRMS

	Healthy Controls (Mean $\pm$ SD)	RRMS (Mean $\pm$ SD)	% Decrease (Controls vs. RRMS)	Effect Size Cohen's <i>d</i>	P-value
CCA	5.36 $\pm$ 0.64	4.29 $\pm$ 0.73	20.1%	0.62	<0.001
BPF	0.846 $\pm$ 0.015	0.826 $\pm$ 0.032	2.3%	0.39	0.004
GMF	0.527 $\pm$ 0.022	0.517 $\pm$ 0.016	2.0%	0.20	0.036
WMF	0.318 $\pm$ 0.020	0.310 $\pm$ 0.022	2.8%	0.22	0.222

Key: CCA = normalized corpus callosum area, BPF = brain parenchymal fraction, GMF = gray matter fraction, WMF = white matter fraction, RRMS = relapsing-remitting multiple sclerosis.